Turkish Journal of Earth Sciences

http://journals.tubitak.gov.tr/earth/

Research Article

Turkish J Earth Sci
(2020) 29: 139-153
© TÜBİTAK
doi:10.3906/yer-1907-5

Eocene-Oligocene succession at Kıyıköy (Midye) on the Black Sea coast in Thrace

Aral I. OKAY[1,2,*], Michael D. SIMMONS[3], Ercan ÖZCAN[2], Stephen STARKIE[4], Michael D. BIDGOOD[5], Andrew R.C. KYLANDER-CLARK[6]

[1]Eurasia Institute of Earth Sciences, İstanbul Technical University, İstanbul, Turkey
[2]Department of Geology, Faculty of Mines, İstanbul Technical University, İstanbul, Turkey
[3]Halliburton, Milton Park, Abingdon, United Kingdom
[4]Datum Stratigraphic Associates Limited, Chorltonville, Manchester, United Kingdom
[5]GSS Geoscience Ltd., Oldmeldrum, Aberdeenshire, United Kingdom
[6]Department of Earth Sciences, University of California Santa Barbara, Santa Barbara, CA, USA

Received: 02.07.2019 • **Accepted/Published Online:** 18.08.2019 • **Final Version:** 02.01.2020

Abstract: A belt of Upper Eocene–Lower Oligocene marine sedimentary rocks extends from Kıyıköy on the Black Sea coast to Pınarhisar in the Thrace Basin, suggesting a marine connection between the Black Sea and the Thrace Basin during this period. The Cenozoic succession of this marine corridor was studied in the vicinity of Kıyıköy along two measured stratigraphic sections. The sequence lies unconformably over metamorphic basement rocks and consists of ~75 m of bioclastic limestone and sandstone of the Soğucak Formation, overlain by ~40 m of limestone, marl, mudstone, sandstone, and acidic tuff, which are assigned to the newly defined Servez Formation. Larger benthic foraminifera indicate that the lower part of the succession is Late Eocene in age, and nannoplankton from the upper part of the succession suggest an Early Oligocene age; these age determinations are also supported by the Sr-isotope data. A U-Pb age from zircons from a tuff bed is 33.9 ± 0.4 Ma, which falls on the Eocene–Oligocene boundary. The Kıyıköy Upper Eocene–Lower Oligocene sequence was deposited in shallow marine conditions below 50-m water depth. The depositional setting, as well as the relatively reduced thickness of the sequence, shows that any marine connection between the Black Sea and the Thrace Basin along the Kıyıköy-Pınarhisar corridor was not significant. The Late Eocene–Early Oligocene marine connection between the Black Sea and the Thrace Basin occurred along the Çatalca gap southeast of Kıyıköy. In the Çatalca gap the Upper Eocene–Lower Oligocene sequence is much thicker (350 m) and was deposited at much greater water depth.

Key words: Thrace Basin, Black Sea, Eocene, Oligocene, foraminifera, nannoplankton

1. Introduction

At the end of the Eocene, most of the Balkans, Anatolia, and Iran constituted a land area that divided the Tethys marine realm into the Black Sea–Caspian in the north and the Eastern Mediterranean in the south (Figure 1; e.g., Lüttig and Steffens, 1976; Popov et al., 2004). Because of tectonic uplift and eustatic sea-level fall, increasing isolation of the Black Sea–Caspian from the open oceans led to the formation of the Paratethys in the Oligocene and Miocene with periodically restricted marine conditions (e.g., Rögl, 1999). The Thrace Basin existed as a distinct depocentre during the Eocene and Oligocene on the margin of the Paratethys; it was separated from the Black Sea by the metamorphic rocks of the Strandja Massif (Figure 2). Outcrops of the Eocene–Oligocene sediments in Thrace indicate that there were two possible corridors of connection between the Black Sea and the Thrace Basin, and eventually to the Eastern Mediterranean in this period; the first was through the Çatalca gap west of İstanbul and the second between Kıyıköy and Pınarhisar (Figure 2). Shallow marine Middle-Upper Eocene (Bartonian–Priabonian) limestones (the Soğucak Formation) and overlying open marine uppermost Eocene–Lower Oligocene marls (the İhsaniye Formation) in the Çatalca gap indicate a marine connection between the Black Sea and the Thrace Basin during the Late Eocene and Early Oligocene (Akartuna, 1953; Okay et al., 2019b). The second possible corridor is suggested by geological maps, which show a wide belt of Eocene limestones extending from the Black Sea coast at Kıyıköy, formerly Midye, southwest to the Pınarhisar in the Thrace Basin (Figure 2; Çağlayan and Yurtsever, 1998; Türkecan and Yurtsever, 2002). Most of this region is heavily forested with few continuous outcrops; the best outcrops are located along the Black Sea coast, which

* Correspondence: okay@itu.edu.tr

This work is licensed under a Creative Commons Attribution 4.0 International License.

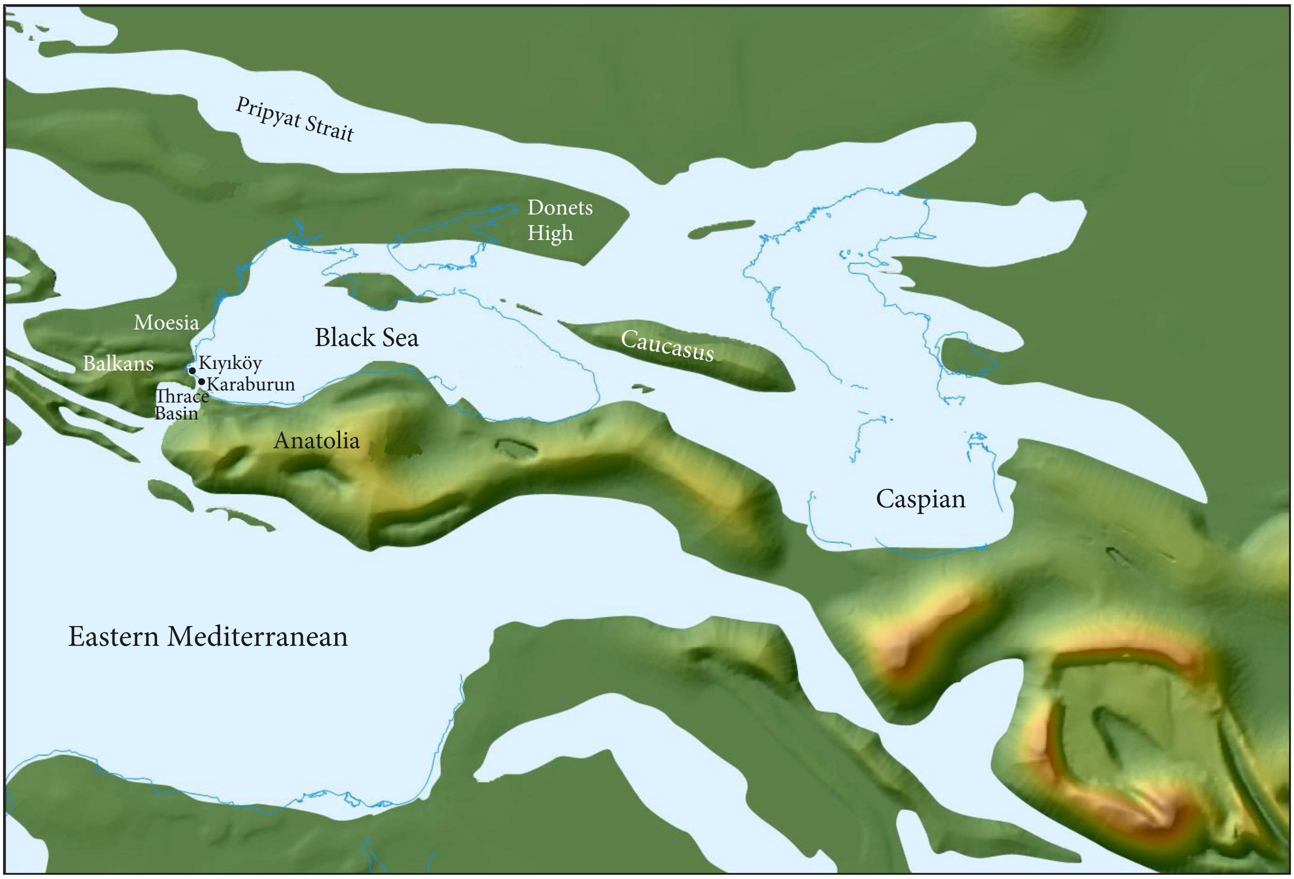

Figure 1. Simplified regional palaeogeographic setting of the Early Oligocene of the Eastern Paratethys, modified and synthesised after various sources, most notably Popov et al. (2004).

also exposes the contacts between the metamorphic basement and the overlying Eocene series. We studied the coastal part of the Eocene–Oligocene section near Kıyıköy to establish its stratigraphy, determine the age of marine transgression over the metamorphic rocks of the Strandja Massif, and establish possible marine gateways between the Black Sea and the Thrace Basin. Previously the Eocene–Oligocene succession in the Kıyıköy area was studied by Varol et al. (2009) with a short stratigraphic description and comments on the fauna present.

2. Geological setting

The Black Sea opened as a back-arc basin during the Late Cretaceous (e.g., Görür, 1988), and since then, it has been a site of continuous deposition, resulting in sedimentary thicknesses of over 10 km (e.g., Nikishin et al., 2015). The Thrace Basin is a more recent depocentre; it formed in the Middle to Late Eocene (Bartonian to Priabonian) and was partially inverted in the Late Oligocene–Early Miocene (Turgut et al., 1991; Siyako and Huvaz, 2007; Okay et al., 2010). The base of the Thrace Basin sequence is marked by shallow marine limestones of the Middle-Upper Eocene (Bartonian–Priabonian) Soğucak Formation (Özcan et al., 2010, 2018; Less et al., 2011; Yücel et. al., 2020). The Soğucak Formation is usually less than 70 m thick, and it lies unconformably over the metamorphic rocks of the Strandja Massif and over the Palaeozoic sediments of the İstanbul Zone. In the centre of the Thrace Basin, the Soğucak Formation is overlain by a thick (>5 km) Upper Eocene to Oligocene clastic sequence ranging from distal turbidites to deltaic deposits with lignite seams. Gentle folding and uplift occurred at the end of the Oligocene and in the Early Miocene, which was followed by renewed deposition of continental sands in the Miocene and Pliocene.

The Strandja Massif constitutes most of the basement to the Thrace basin. The Strandja Massif was deformed and metamorphosed during the latest Jurassic to earliest Cretaceous (Okay et al., 2001; Sunal et al., 2011), exhumed in the Late Cretaceous (Cattò et al., 2018), and unconformably overlain by Upper Cretaceous sedimentary and volcanic rocks, which are preserved on its north-eastern margin at İğneada on the Black Sea coast. The Late Cretaceous transgression starts with

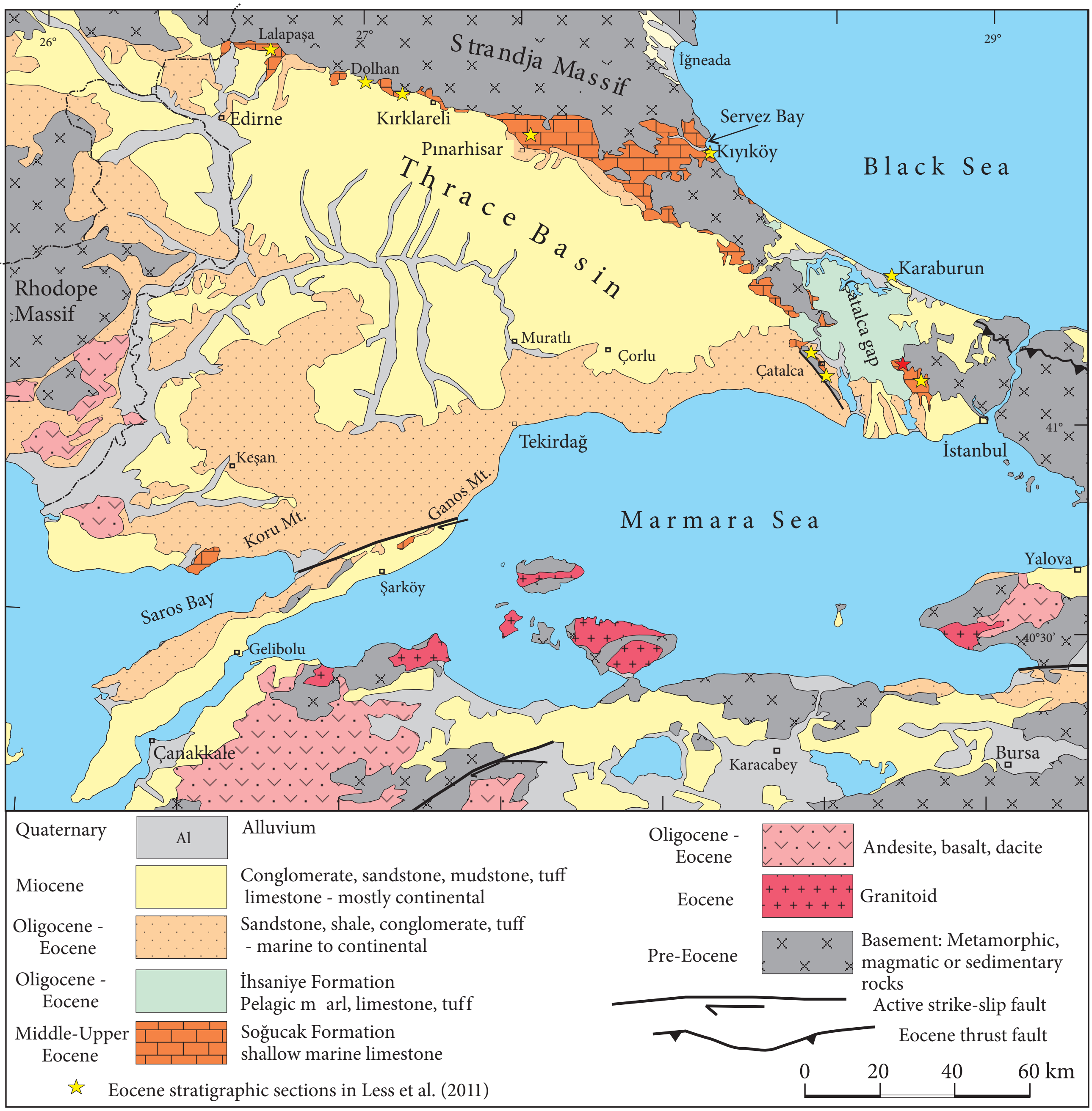

Figure 2. Geological map of the Thrace region (compiled from Türkecan and Yurtsever 2002; Okay et al., 2010).

Cenomanian sandy limestones and passes up into a volcaniclastic-volcanic series, which constitutes part of the Late Cretaceous Pontide-Sredna-Gora magmatic arc (Okay et al., 2001). After the Early Eocene, the Strandja Massif formed a palaeogeographic high separating the Black Sea from the Thrace Basin (Figure 2). The high was breached apparently in two regions: in the Kıyıköy-Pınarhisar corridor, and in the Çatalca gap (Okay et al. 2019b).

3. Geology and stratigraphy of the Kıyıköy region

The basement in the Kıyıköy region is made up of the phyllite, quartz-micaschist, calc-schist, and metagranites of the Strandja Massif, which are unconformably overlain by a Cenozoic shallow marine sedimentary sequence (Figure 3; Varol et al., 2009). The basal unconformity is best exposed in the axis of the Kazandere dam, where metagranites are overlain by yellowish-red conglomerate and sandstone with granite clasts, these sediments being

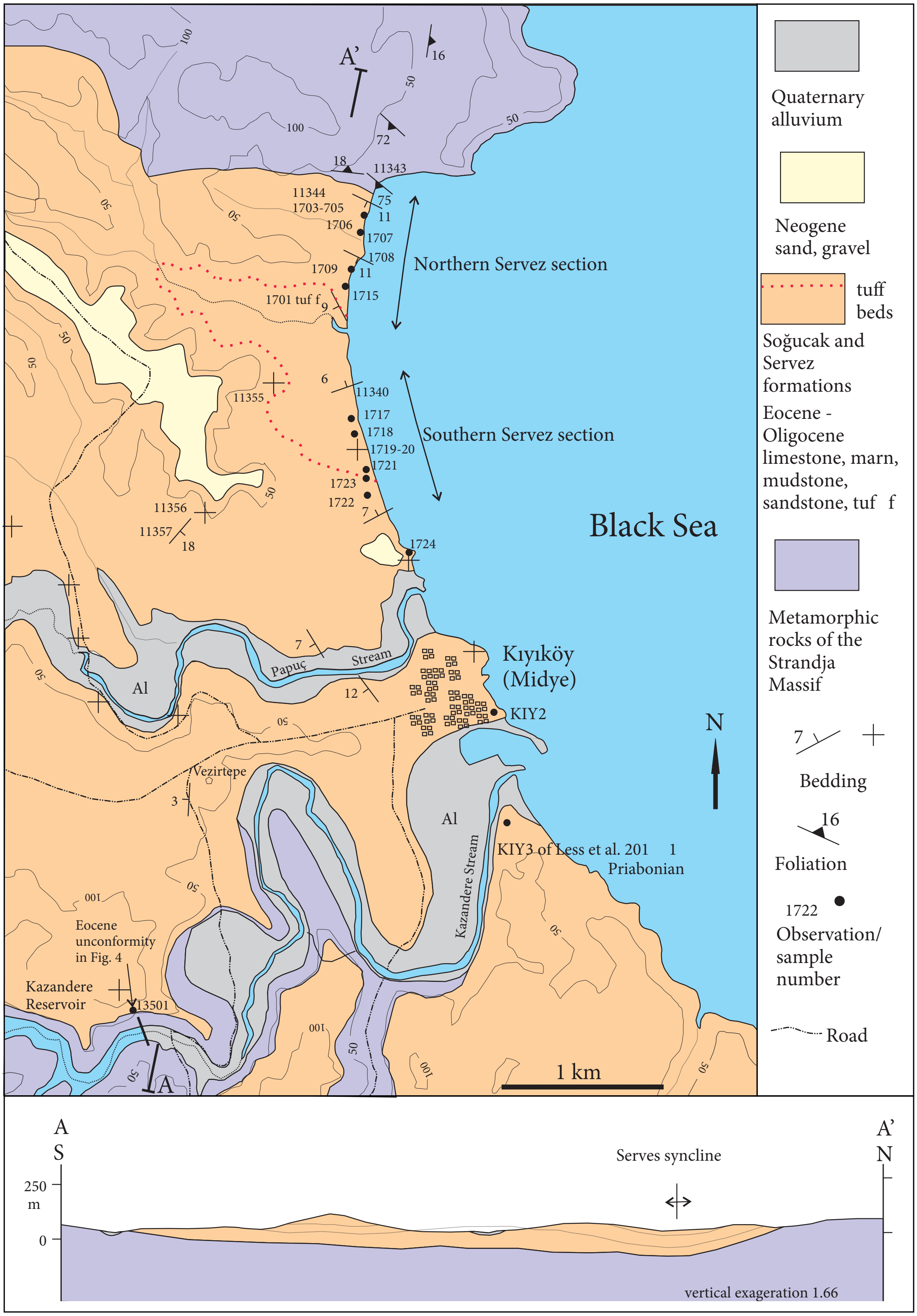

Figure 3. Geological map of the Kıyıköy (Midye) region. For location see Figure 2.

of presumably Late Eocene age (Figure 4). This basal clastic section is up to 6 m in thickness and pinches out laterally. It is overlain by a 20-m-thick sequence of lithified bioclastic limestones intercalated with poorly cemented carbonate-rich sandstones (Figure 4). The limestones contain abundant quartz clasts (1–2 mm), bivalve and gastropod fragments, and Miliolidae, but other, potentially more age-significant, foraminifera are absent.

A more complete Cenozoic succession is exposed at Servez Bay, north of Kıyıköy along a 2-km-long coastal section (Figure 3). At Servez Bay, the Eocene–Oligocene section forms a gentle syncline with an east-west trending

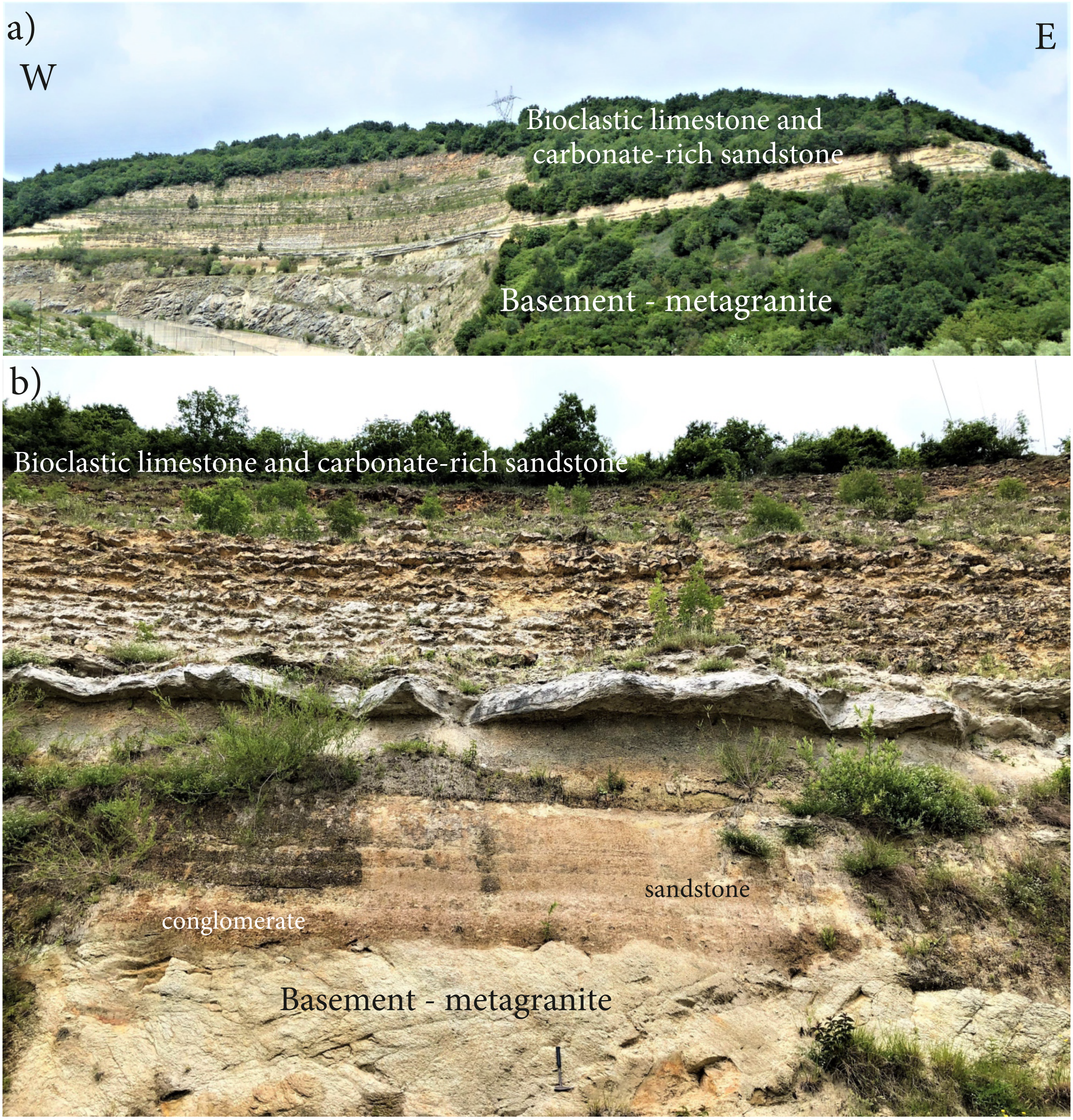

Figure 4. Panoramic and close-up views of the basement/Eocene unconformity. The metagranites of the Strandja Massif are unconformably overlain by conglomerate and sandstone, which pass up into calc-arenite and carbonate-rich sandstones. Axis of the Kazandere dam (locality 13501, UTM 35 T 05 89 600 – 46 07 995).

fold axis. We have measured stratigraphic sections both on the northern and southern limbs of the syncline (Figure 5). The metamorphic rocks are exposed on the northern end of Servez Bay and consist of metadiorite, phyllite, and calc-schist (Figure 6a). Following a 50-m gap with no outcrop, the Eocene–Oligocene section starts with an intercalation of medium-bedded, black sandstone and bioclastic limestone beds showing large-scale cross-bedding (Figure 6b); these are overlain by a 20-m-thick sequence of bioclastic sandy limestones with a few bluish-green sandstone and siltstone beds. The bioclastic limestones, which are the dominant lithology in the first 75 m of the Northern Servez section, are typically yellowish grey, pale yellow, and showing irregular wavy and medium bedding (Figure 6c). In the lower part of the succession they contain abundant coral, bivalve, gastropod, echinoid,

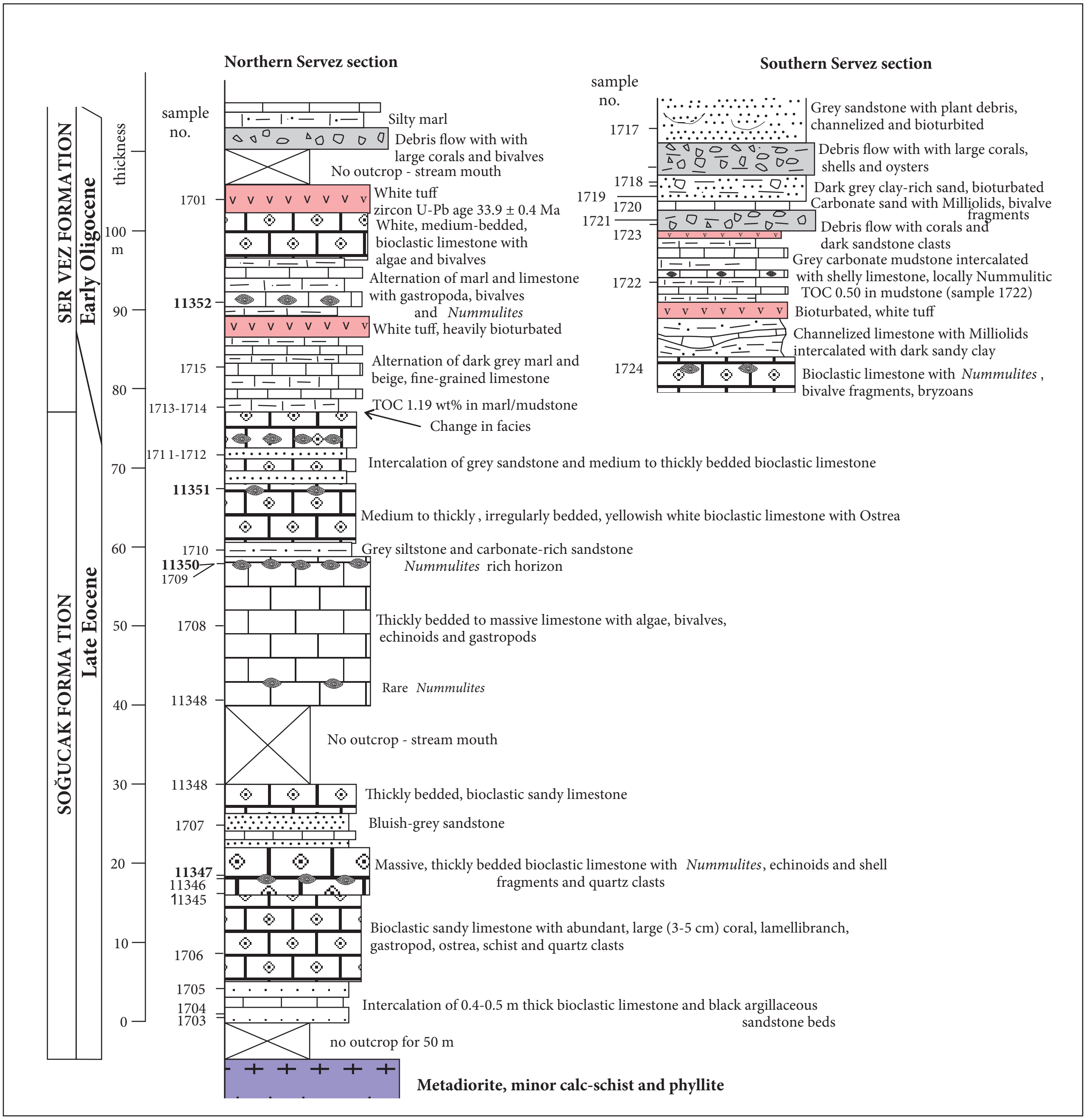

Figure 5. Measured stratigraphic section in the northern limb and the southern limb of the syncline in the Servez Bay – Northern and Southern Servez sections. The interpreted Eocene–Oligocene boundary is uncertain within about 10 m. For location see Figure 3.

Figure 6. Field photographs from the Northern Servez section. a) General view of the Northern Servez section. b) Cross-bedded limestone and sandstone at the base of the Servez section. c) Bioclastic limestones, which characterise much of the lower part of the Servez section. They are typically irregularly, medium to thickly bedded, and contain abundant macrofossils and algae and locally *Nummulites*-rich horizons. d) Close-up view of the *Nummulites*-rich horizon in the bioclastic limestones. The diameter of the coin is 2.5 cm. e) Alternation of dark grey marl and planar bedded limestone; marls are characterised by high TOC content (1.19 wt.% in sample 1713). f) Upper tuff bed at the top of the Northern Servez section. g) The Oligocene echinoid *Scutella subtrigona* from the top part of the Northern Servez section.

oyster, and calcareous algae fragments; schist and quartz pebbles derived from the basement are also common. There are several *Nummulites*-rich horizons within the bioclastic limestones (Figure 6d). At 76 m above the base of the Northern Servez section there is a sharp change in facies from bioclastic limestones to an alternation of dark grey marl and fine- to medium-grained planar bedded limestone devoid of any macrofossils (Figure 6e). Marls directly above this facies change have an elevated total organic carbon (TOC) content (1.19 wt.% in sample 1713). The marl-limestone series are overlain by a 2.5-m-thick, highly bioturbated, biotite-bearing, white tuff (Figure 6f), which is followed by more alternations of marl and limestone; the limestone beds above the tuff horizon are more bioclastic and contain algae, gastropods, echinoids, bivalves, and *Nummulites*. The echinoids include a sand dollar tentatively identified as *Scutella subtrigona*, a species originally described from the Oligocene of Romania (Koch, 1884, Figure 6g). The bioclastic limestones are overlain by a second white tuff horizon.

The continuation of the Northern Servez section can be observed in the Southern Servez section on the southern limb of the syncline; the two tuff horizons provide precise correlation between the sections (Figure 5). The Southern Servez section starts with *Nummulites*-bearing bioclastic limestones and sandy marls, which are overlain by the first tuff bed (Figure 7a). The tuff is itself overlain by dark grey mudstone beds intercalated locally with *Nummulites*-bearing bioclastic limestones (Figure 7b). A sample from the dark grey mudstones (1722) has a TOC content of 0.50 wt.%. The mudstone-limestone succession is overlain by the second tuff bed. Above the second tuff bed there are debris flow horizons with large corals (up to 1 m across) and bivalve (including oyster) clasts in a sandy marl matrix (Figure 7d). Bioturbated, channelised, carbonate-rich argillaceous sandstone beds occur between the debris flow horizons.

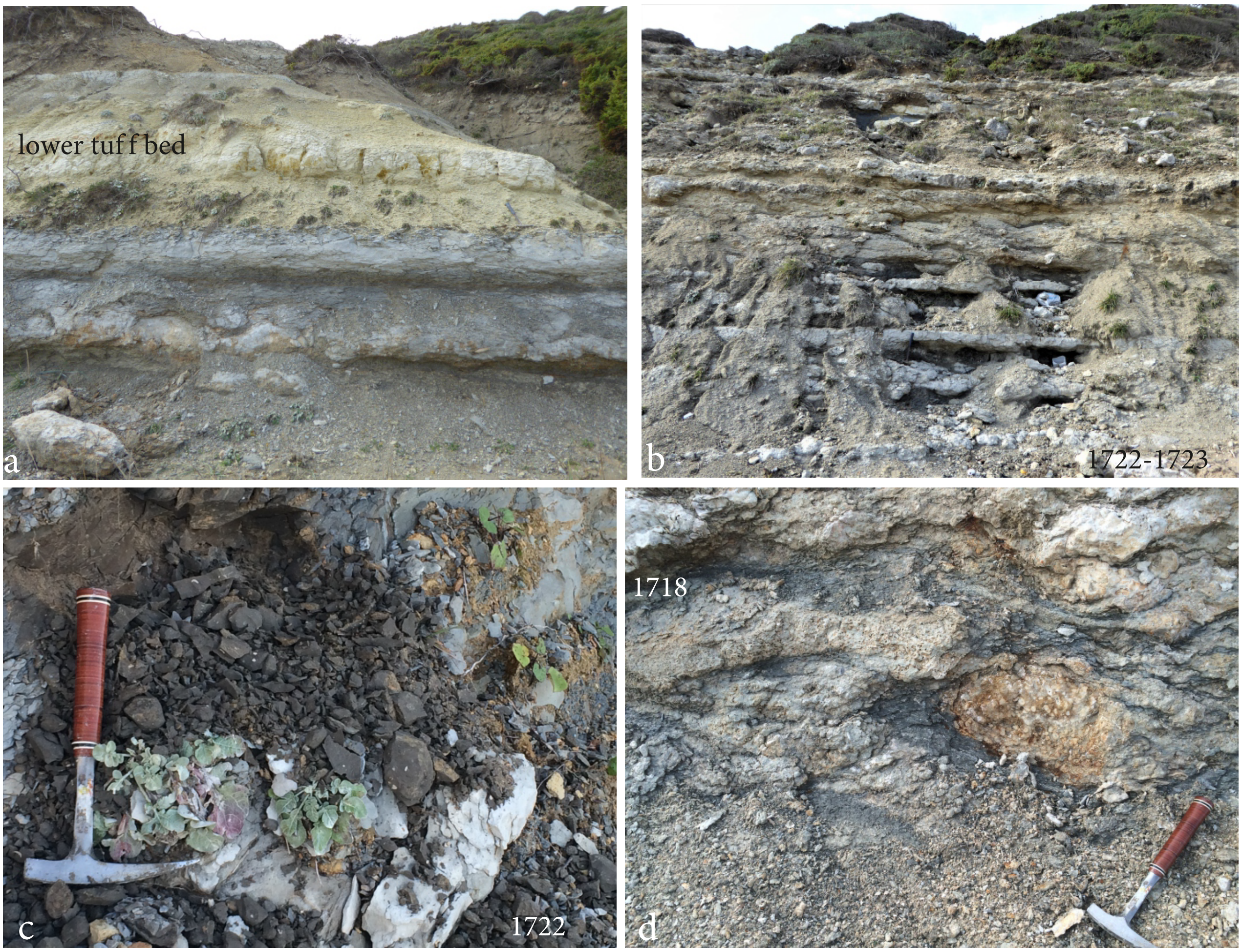

Figure 7. Field photographs from the Southern Servez section. a) Lower tuff bed overlying dark argillaceous sandstone and limestone beds. b) Intercalation of dark grey mudstone and bioclastic limestone. c) Close-up view of the dark mudstones, which have yielded a TOC value of 0.50 wt.% (sample 1722). d) Debris flow horizon with blocks of corals.

The Southern Servez section is bounded in the south by the alluvial plain of the Papuç Stream (Figure 3). South of the alluvium, there is a 40-m sequence of thick bioclastic limestones, corresponding to the lower part of the Northern Servez section; these limestones were sampled by Less et al. (2011).

4. Biostratigraphy and palaeoenvironment of the Kıyıköy Eocene–Oligocene sequence

Samples from both the Northern and Southern Servez sections were analysed for their foraminiferal and calcareous nannofossil content to provide information on likely age and depositional setting. Selected samples were also studied for Sr isotopes and zircons from a tuff bed were isotopically dated. Previously, some of the oldest part of the Kıyıköy sedimentary succession was shown to be of Late Eocene age based on the presence of *Nummulites budensis* in one of the samples studied by Less et al (2011). Sample KIY3 (Figure 3) comes from the bioclastic limestones, which lie stratigraphically below the base of our Southern Servez section (Figure 3). Varol et al. (2009) described four stratigraphic sections of Late Eocene–Early Oligocene age from the Kıyıköy region; however, as the locations of the sections are not given, they are difficult to correlate with the Servez sections.

4.1. Calcareous nannofossils

Among the microfossils present in the succession, the calcareous nannofossils provide the most definitive insight in terms of age control. Biozone NP21 (Martini, 1971) straddles the Eocene/Oligocene boundary and is defined as the interval between the last (youngest) occurrence (LO) of *Discoaster saipanensis* at its base and the LO of *Coccolithus formosus* at its top. This zone was recently subdivided by Agnini et al. (2014) into CNE21 (*Helicosphaera compacta* Partial Range Zone) and CNO1 (*Ericsonia formosa*/*Clausiococcus subdistichus* Concurrent Range Zone). CNE21 corresponds with the lower (Late Eocene) part of NP21, whereas CNO1 corresponds with the upper (Early Oligocene) part of NP21. A significant increase in the abundance of *Clausiococcus subdistichus* defines the base of CNO1.

In the Southern Servez section, sample 1722 contains high percentages of *C. subdistichus* and, in the absence of clearly Eocene taxa, can thus be attributed to Subzone CNO1, the Early Oligocene part of NP21. Samples above this in this section (i.e. up to 1718) have few *C. subdistichus* but still seem compatible with an assignment to CN01.

In the Northern Servez section, there is no *C. subdistichus* acme and the section seems harder to constrain. Nonetheless, in sample 1711 the presence of *C. subdistichus*, *C. formosus*, and *Lanternithus minutus* and the absence of obviously Eocene taxa is suggestive of biozone NP21, if not explicitly Subzone CN01. At 1710 and below, samples appear to contain more dominantly Eocene taxa (e.g., *D. saipanensis*), suggestive of the lower part of NP21 (CNE21) or NP20. However, preservation is poor and it is not possible to rule out that reworking has taken place. Presumably reworked Eocene taxa also occur in samples 1711 and above. The proximal depositional setting as determined by the foraminiferal assemblages can explain the low abundance and diversity of the nannofossil assemblages and their poor preservation.

4.2. Larger benthic foraminifera

The Northern Servez section yielded abundant but nondiverse larger benthic foraminiferal (LBF) assemblages occurring mainly in limestone beds. The weakly cemented limestone beds permit the collection of loose specimens that are necessary for the preparation of equatorial sections and biometric study of LBF. The LBF were studied in four levels in samples 11347, 11350, 11351, and 11352 from an interval of ca. 70 m (Figure 5); they are characterised by only reticulate and radiate *Nummulites*, and *Operculina* (Figure 8). Orthophragminids and other characteristic Eocene LBF taxa such as *Heterostegina*, *Spiroclypeus*, *Assilina*, *Pellatispira*, *Calcarina*, and *Orbitolite*s are not present. The most common LBF group is formed by reticulate *Nummulites* occurring in all samples, though they are subordinate in sample 11347 and most abundant in sample 11350. These specimens display heavy reticulation (Figures 8H and 8J) and lack irregular mesh-like external features. The Eocene reticulate *Nummulites* differ from Oligocene ones by having reticulation rather than irregular mesh, though the transition between them is not sharp and this criterion is not reliable in the differentiation of *Nummulites fabianii* and *Nummulites fichteli* (see Özcan et al., 2019 for the subdivision of *N. fabianii* lineage and test features). The average proloculus diameters of reticulate *Nummulites* from all samples are larger than 200 µm (Table 1). This and the external test features suggest that these specimens represent *N. fabianii* (Prever in Fabiani, 1905). Typically, *N. fabianii* is a Late Eocene species and *N. fichteli* is an Oligocene species (e.g., Racey, 1995), but recently Less et al. (2006), Özcan et al. (2009), and Less and Özcan (2012) have suggested that *N. fabianii* also occurs in Early Oligocene strata and *N. fitchteli* in Late Eocene strata.

Operculina only occurs sporadically in sample 11347. Radiate *Nummulites* are present in all samples. These specimens lack reasonable variation in their equatorial sections and were tentatively assigned to *Nummulites* cf. *incrassatus*.

Larger benthic foraminifera indicate a Late Eocene–Early Oligocene age range for the Northern Servez section based on the presence of heavily reticulated *N. fabianii* and occurrence of *N.* cf. *incrassatus*. More definite Oligocene *Nummulites* such as *Nummulites vascus*, present at Karaburun to the south-west of Kıyıköy (Sakınç 1994; Less

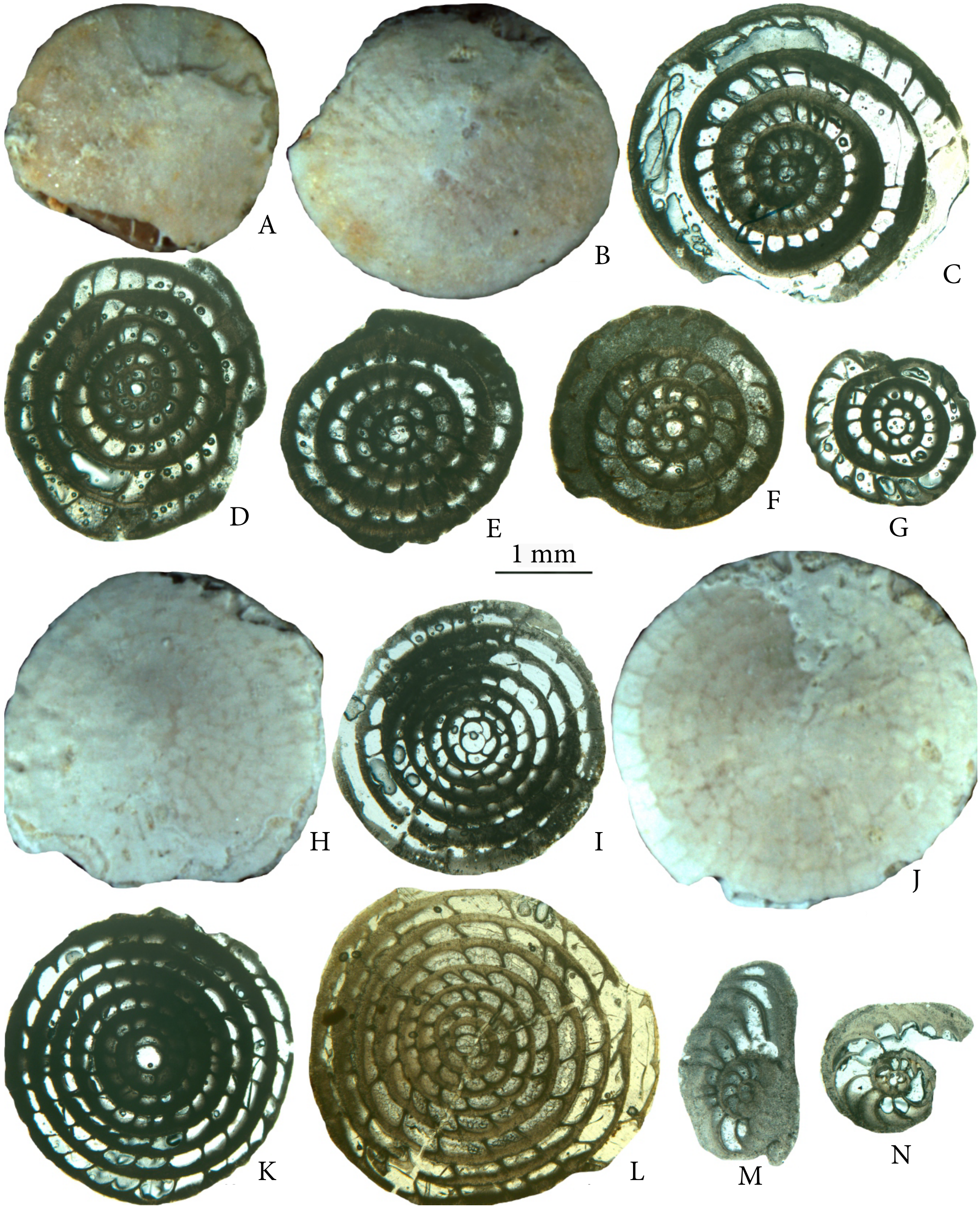

Figure 8. External features and equatorial sections of radiate (A–G) and reticulate *Nummulites* (H–L) and equatorial sections of *Operculina* specimens (M–N) from the Northern Servez section. A–B, D–G: *Nummulites* cf. *incrassatus* de la Harpe, 1883, C: *Nummulites* sp., H–L: *Nummulites fabianii* (Prever in Fabiani, 1905), M–N: *Operculina* sp., late Eocene/early Oligocene transition. A: 11352-8, B–C: 11352-5, D: 11350-26, E: 11350-27, F: 1350-29, G: 11350-17, H: 11352-1, I: 11350-38, J: 11352-2, K: 11350-43, L: 11350-32, M: 11347-4, N: 11347-7.

et al., 2011), or Eocene *Nummulites* such as *N. budensis* as previously recorded by Less et al. (2011) from Kıyıköy, have not been noted in the material studied.

4.3. Planktonic and benthic foraminifera, and ostracods

Planktonic foraminifera are almost absent from the studied material (single specimens in 1711 and 1713).

Small calcareous benthonic foraminifera and ostracods are sporadically common in some samples, but are not especially age-significant. The only ostracod that can be confidently identified by reference to the published literature is *Cytheridea pernota*, which has a Late Eocene to Early Oligocene range (Şafak, 2016). Among the more common calcareous benthonic foraminifera are *Baggina dentata*, *Hoeglundina elegans* (sample 1710), and *Pararotalia lithothamnica* (sample 1718). These have been recorded from Early Oligocene strata at Karaburun (Simmons et al., 2020) to the south-east of Kıyıköy, but have generally long stratigraphic ranges, such that they are not conclusively Early Oligocene indices.

4.4. Isotopic data

Two tuff beds occur in the upper part of the Servez sections. Zircons were separated from the upper tuff bed and were dated using U-Pb ICP-MS laser ablation method at the University of California Santa Barbara. The methods of mineral separation and dating are given by Okay et al. (2019a) and the analytical data are given in Table 2. The

Table 1. Biometric features of the reticulate *Nummulites* in Servez Bay. N: number of studied samples.

Sample	N	Proloculus diameter, range (μm)	Proloculus diameter, mean (μm)
11350	41	220–340	266.6
11351	10	170–300	234.0
11352	3	250–290	265.0

Table 2. U-Pb isotopic geochronological data from zircons from the acidic tuff sample 1701.

Grain	U pp m	Th pp m	^{207}Pbf/ ^{235}U	2s	^{206}P b/ ^{238}U	2s	rho	^{238}U/ ^{206}pb	2s	^{207}Pb/ ^{206}Pb	2s	rho	^{208}Pb/ ^{232}Th	2s	Best age	2s	Concordance
1	597	691	0.159	0.012	0.01	0.00	0.92	161.29	10.15	0.185	0.007	0.49	0.004	0.000	32.9	2.1	0.27
2	475	758	0.037	0.001	0.01	0.00	0.63	192.68	7.08	0.053	0.002	0.46	0.002	0.000	33.1	1 .2	0.90
3	272	289	0.081	0.013	0.01	0.00	0.70	179.21	8.50	0.104	0.014	0.26	0.002	0.000	33.3	1.7	0.45
4	210	186	0.304	0.030	0.01	0.00	0.98	132.28	6.19	0.295	0.020	0.40	0.008	0.001	33.3	2.2	0.18
5	385	400	0.036	0.002	0.01	0.00	0.69	191.57	7.32	0.049	0.002	0.43	0.002	0.000	33.5	1 .3	0.95
6	209	164	0.035	0.003	0.01	0.00	0.65	191.57	9.61	0.049	0.003	0.34	0.002	0.000	33.5	1.7	0.96
7	194	145	0.036	0.003	0.01	0.00	0.65	191.20	9.91	0.050	0.003	0.50	0.002	0.000	33.5	1.7	0.93
8	530	909	0.134	0.017	0.01	0.00	0.74	164.74	7.79	0.158	0.014	0.30	0.003	0.000	33.5	1.8	0.31
9	266	164	0.081	0.015	0.01	0.00	0.89	1 77.94	8.39	0.103	0.016	0.24	0.003	0.000	33.6	1 .8	0.46
10	242	261	0.132	0.025	0.01	0.00	0.88	164.74	11.35	0.155	0.020	0.30	0.003	0.000	33.7	2.5	0.31
11	279	337	0.035	0.002	0.01	0.00	0.49	190.11	9.47	0.049	0.003	0.38	0.002	0.000	33.7	1.7	0.97
12	819	976	0.039	0.002	0.01	0 00	0.49	187.97	7.09	0.054	0.002	0.39	0.002	0.000	33.9	1.3	0.89
13	264	223	0.120	0.009	0.01	0.00	0.72	166.67	7.45	0138	0.007	0.46	0.004	0 000	34.1	1.6	0.34
14	293	263	0.040	0.003	0.01	0.00	0.58	186.92	6.72	0.052	0.003	0.30	0.002	0.000	34.2	1 .2	0.87
15	139	164	0.570	0.060	0.01	0.00	0.72	99.60	7.32	0.417	0.025	0.42	0.010	0.001	34.3	3.8	0.14
16	161	141	0.062	0.013	0.01	0.00	0.68	177.62	13.41	0.084	0.017	0.17	0.002	0.000	34.5	2.7	0.59
17	178	160	0.053	0.009	0.01	0.00	0.52	179.86	8.26	0.074	0.012	0.27	0.002	0 000	34.5	1.7	0.68
18	79	62	0.072	0.016	0.01	0.00	0.77	175.75	8.77	0.091	0.018	0.21	0.003	0.000	34.5	1.9	0.52
19	178	147	0.040	0.003	0.01	0.00	0.75	184.50	10.54	0.053	0.004	0.33	0.002	0.000	34.6	2.0	0.88
20	244	210	0.039	0.003	0.01	0.00	0.75	182.15	7.86	0.051	0.003	0.47	0.002	0 000	35.1	15	0.91
21	79	80	0.042	0.003	0.01	0.00	0.45	176.68	10.30	0.053	0.005	0.35	0.002	0.000	36.1	2.1	0.88
22	115	85	0.545	0.035	0.01	0.00	0.92	98.81	6.46	0.395	0.012	0.49	0.016	0.001	36.3	3.1	0.15
23	200	249	0.420	0.160	0.01	0.00	1.00	116.28	19.07	0.306	0.038	0.40	0.007	0.002	37.1	6.7	0.16
24	1060	8	0.089	0.005	0.01	0.00	0.98	75.08	4.65	0.048	0.001	0.35	0.006	0.001	85.2	5.3	0.99

average age is 33.9 ± 0.4 Ma (Figure 9). The International Chronostratigraphic Chart 2018 places the Eocene–Oligocene boundary at 33.9 Ma (e.g., Ogg et al., 2008; Cohen et al., 2013). However, recent geochronological work at the Eocene–Oligocene type boundary section indicates a slightly older age of 34.09 ± 0.08 Ma for the boundary (Sahy et al., 2017). Regardless, the tuff bed was deposited at ages approximating to the Eocene-Oligocene boundary.

Given some uncertainties in the biostratigraphy-based age calibration of the sedimentary succession at Kıyıköy, a small selection of limestone samples were analysed for their $^{87}Sr/^{86}Sr$ values using the procedures described in this issue of the journal by Tulan et al. (2020). The results were converted to numerical ages with reference to the data compilation of McArthur et al. (2012). Sample 1708 from a massive limestone in the lower part of the Northern Servez section yields a $^{87}Sr/^{86}Sr$ value of 0.707798, which calibrates to an age of 34.8 ± 0.7 Ma, Late Eocene, late Priabonian. This is supportive of the conclusions from the study of nannofossils and of the results from Less et al. (2011) that this part of the section is Late Eocene in age. Sample 1720 from a miliolid-rich carbonate sand in the Southern Servez section, and high in the stratigraphy, yields a $^{87}Sr/^{86}Sr$ value of 0.707886, which calibrates to an age of 32.7 ± 0.7 Ma, Early Oligocene, early Rupelian. This is supportive of the conclusions from nannofossil analysis and radiometric isotope analysis of tuffs lying below this sample. However, although these data appear useful in determining the age calibration of the Kıyıköy section, caution should be expressed because as demonstrated by Tulan et al. (2020) $^{87}Sr/^{86}Sr$ values from some age-equivalent sediments in the Western Black Sea Basin are demonstrably discordant with the global $^{87}Sr/^{86}Sr$ signal, presumably because of local influences on sea-water chemistry.

4.5. Palaeoenvironment

In terms of palaeoenvironments, samples 1703–1706 from the lower part of the northern limb of the syncline contain too sparse a fauna to make a conclusive determination. All other samples from the northern and southern limbs contain moderately abundant and diverse calcareous benthonic foraminifera such as *Nonion commune*, some

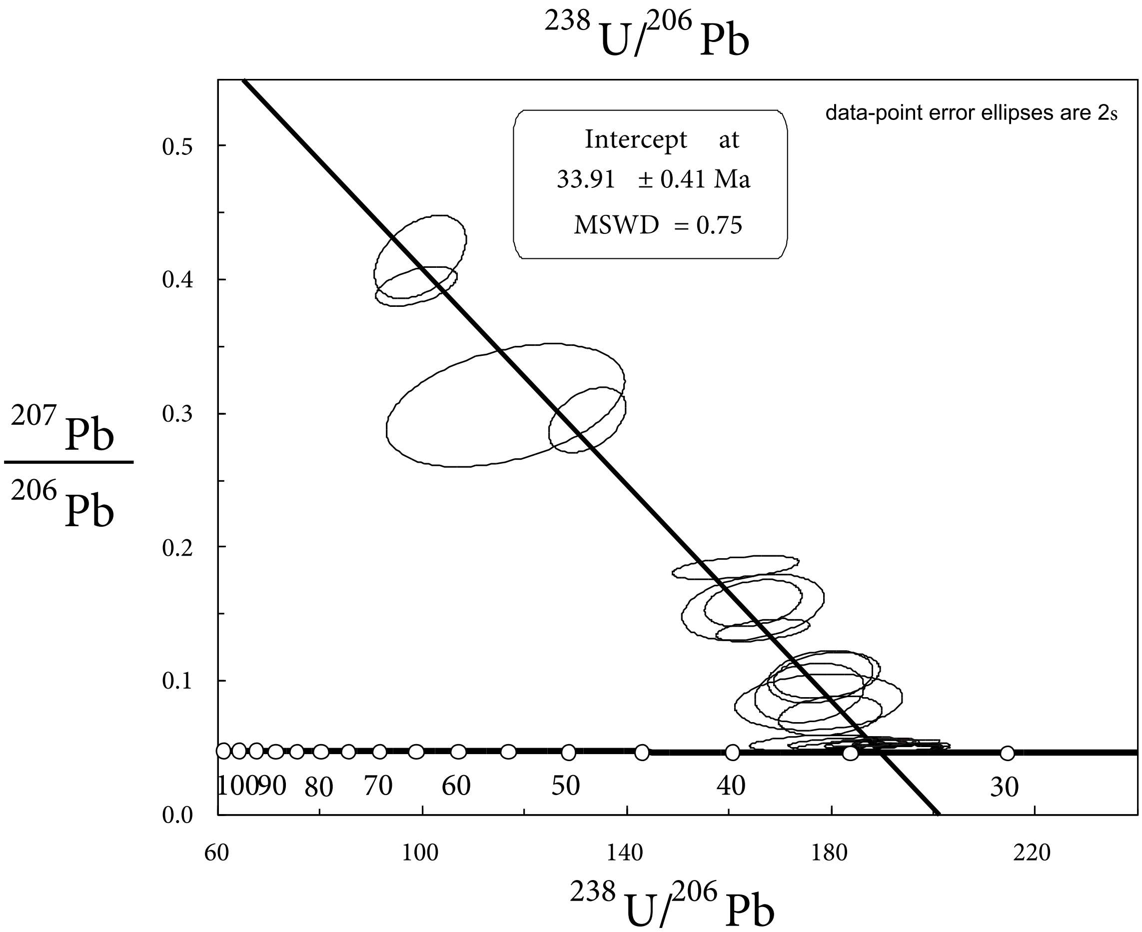

Figure 9. U-Pb zircon concordia diagram from the upper acidic tuff bed from the Northern Servez section.

"larger" rotaliids, and elphidiids that suggest a shallow marine palaeoenvironment. The lack of planktonic foraminifera suggests water depths less than 50 m while the presence of larger foraminifera that host symbiotic algae (e.g., *Nummulites*) suggests water depths within the photic zone (perhaps <25 m). The ostracod *Cytheridea*, which is common in many samples, is regarded as a lagoonal–littoral species by Safak (2016).

5. Lithostratigraphy

The basal sedimentary levels of the Thrace Basin are characterised by massive, thickly bedded, shallow marine Middle-Upper Eocene limestones with rich micro- and macrofauna, which are assigned to the Soğucak Formation (Siyako, 2006; Özcan et al., 2010; Less et al., 2011). In the centre of the Thrace Basin the Soğucak Formation is overlain by a regressive siliciclastic sequence, several thousands of meters thick (e.g., Turgut et al., 1991; Siyako and Huvaz, 2007). This sequence is named as the Keşan Formation and/or the Ceylan Formation. The Keşan Formation is a thick Upper Eocene–Lower Oligocene turbidite sequence of sandstone and shale and crops out in the Ganos and Koru Mountains (Figure 2). Its type section is in Ganos Mountain (Siyako, 2006). The Ceylan Formation is a poorly defined unit with no type section; it is described as being composed of "pelagic shale, marl, argillaceous limestone, turbiditic sandstone-shale, tuff and olistostromes" (Siyako, 2006).

The Soğucak Formation extends to the margins of the Thrace Basin, where it lies unconformably over the metamorphic rocks of the Strandja Massif (Figure 2; Less et al., 2011). The Upper Eocene bioclastic limestone-sandstone series at Kıyıköy can be broadly assigned to the Soğucak Formation, although it includes sandstone beds and was deposited in shallower marine conditions than the typical Soğucak Formation. Lithostratigraphic sequences above the Soğucak Formation on the margins of the Thrace Basin, however, are distinctly different than those in the centre. They consist of thin (<50 m), very shallow marine Lower Oligocene limestone, marl, and tuff, as observed at Kıyıköy, also at Pınarhisar on the western end of the Kıyıköy-Pınarhisar corridor. At Pınarhisar, İslamoğlu et al. (2010) described a thin (6 m) sequence of Lower Oligocene shallow marine oolites above the Soğucak Formation.

These thin very shallow marine Lower Oligocene sediments on the margins of the Strandja Massif are different from the thick turbidites of the Keşan Formation, from the pelagic sediments of the Ceylan Formation, and from the uppermost Eocene–Lower Oligocene pelagic marls with acidic tuff and calc-arenite beds of the İhsaniye Formation, and they require a new lithostratigraphic name. We suggest the Servez Formation for the thin Lower Oligocene marginal marine sediments of limestone, marl, and tuff with a type area at Servez Bay.

6. Discussion and conclusions

The Upper Eocene-Lower Oligocene sedimentary sequence at Kıyıköy consists of shallow marine bioclastic limestone, sandstone, mudstone, marl, and tuff. The sequence is less than 150 m thick and lies unconformably over the metamorphic rocks of the Strandja Massif. The base of the sequence is marked by laterally discontinuous conglomerate and sandstone horizon, less than 6 m thick, which is overlain by bioclastic limestones with sandstone intercalations, about 75 m thick. Large benthic foraminifera and Sr-isotope data indicate that the basal bioclastic limestones are Late Eocene in age and are ascribed to the Soğucak Formation (Varol et al., 2009; Less et al., 2011), although it differs in detail from the usual aspect of that formation. The bioclastic limestone–sandstone series are overlain by a 40-m-thick sequence of limestone, marl, mudstone, acidic tuffs, and debris flows. Nannofossils and Sr-isotope data suggest that this part of the sequence is Early Oligocene age. Zircon ages from a tuff bed in this part of the sequence give a U-Pb age of 33.9 ± 0.4 Ma (Figure 9). The conventional lithostratigraphy of the Thrace Basin and Turkish sector of the Western Black Sea Basin is difficult to apply to the Kıyıköy region, especially for the Early Oligocene succession. Therefore, we introduce a new term, the Servez Formation, for the Lower Oligocene sequence of limestone, marl, mudstone, acidic tuffs, and debris flows.

Acidic tuff beds are relatively common in the Oligocene sequence of the Thrace Basin. Geochronological data suggest that their ages encompass the whole of the Oligocene but they are absent in the Eocene (this study; Okay et al., 2019b, unpublished data). Thus, the occurrence of acidic tuff beds can be used as a tool in differentiating Eocene and Oligocene sequences in the Thrace Basin.

The Kıyıköy and Karaburun areas have a similar palaeogeographic and tectonic setting on the margins of the Black Sea (Figures 1 and 2). Although the Upper Eocene Soğucak Formation is encountered in both regions, the overlying sequences are distinctly different. In the Karaburun area and in the Çatalca gap, the Soğucak Formation is overlain by uppermost Eocene–Lower Oligocene pelagic marls with acidic tuff beds, the İhsaniye Formation, with a rich fauna of planktonic foraminifera, and with a thickness of 300 m (Okay et al., 2019b; Simmons et al., 2020). The İhsaniye Formation was mostly deposited offshore in a deep shelf. In contrast, the Lower Oligocene sequence at Kıyıköy, the Servez Formation, consists of shallow marine limestone, marl, and tuff and has a thickness of only 40 m, deposited in water depths of less than 50 m. In Karaburun there is an unconformity characterised by a hardground between the Upper Eocene

Soğucak Formation and the Lower Oligocene İhsaniye Formation (Sakınç, 1994; Okay et al., 2019b; Simmons et al., 2020), whereas the contact between the Soğucak and Servez formations in Kıyıköy, approximating to the Eocene–Oligocene boundary, is transitional.

The thin and very shallow marine Upper Eocene–Lower Oligocene sequence at Kıyıköy suggests that there was no significant marine connection between the Black Sea and the Thrace Basin along the Kıyıköy-Pınarhisar corridor; the main Black Sea–Mediterranean connection appears to have been through the Çatalca gap.

Acknowledgements

The organic geochemistry data were provided by Ocean Grove Ltd. Andrew Racey kindly provided comments on some of the foraminifera. The strontium isotope analysis was conducted at SUERC, East Kilbride, UK, under the supervision of Dr. Ryan Eckhart and the age calibration of the data was kindly performed by Prof. John McArthur of University College London. Comments on echinoderm identification were kindly provided by Dr. Andreas Kroh of the Natural History Museum, Vienna. This study was partly supported by TÜBA.

References

Agnini C, Fornaciari E, Raffi I, Catanzariti R, Pälike H et al. (2014). Biozonation and biochronology of Paleogene calcareous nannofossils from low and middle latitudes. Newsletters on Stratigraphy 47/2: 131-181.

Akartuna M (1953). Çatalca-Karacaköy bölgesinin jeolojisi. İstanbul, Turkey: İstanbul Üniversitesi Fen Fakültesi Monografileri (in Turkish).

Çağlayan MA, Yurtsever A (1998). 1:100 000 Scale Geological Maps and Explanatory Notes, Turkey, Burgaz-A3, Edirne-B2, Burgaz-A4 and Kırklareli-B4, B5, B6 and C6 Sheets and Explanatory Text, No. 20-23. Ankara, Turkey: General Directorate of the Mineral Research and Exploration (in Turkish).

Cattò S, Cavazza W, Zattin M, Okay AI (2018). No significant Alpine-age tectonic overprint of the Cimmerian Strandja Massif (SE Bulgaria and NW Turkey). International Geology Review 60: 513-529.

Cohen KM, Finney SC, Gibbard PL, Fan JX (2013). The ICS International Chronostratigraphic Chart. Episodes 36: 199-204.

Görür N (1988). Timing of opening of the Black Sea basin. Tectonophysics 147: 247-262.

İslamoğlu Y, Harzhauser M, Gross M, Jimenez-Moreno G, Coric S et al. (2010). From Tethys to Eastern Paratethys: Oligocene depositional environments, paleoecology and paleobiogeography of the Thrace Basin (NW Turkey). International Journal of Earth Sciences 99: 183-200.

Less G, Kertész B, Özcan E (2006). Bartonian to end-Rupelian reticulate *Nummulites* of the Western Tethys. Anuário do Instituto de Geociências 29: 344-345.

Less G, Özcan E (2012). Bartonian-Priabonian larger benthic foraminiferal events in the Western Tethys. Austrian Journal of Earth Sciences 105: 129-140.

Less G, Özcan E, Okay AI (2011). Stratigraphy and larger foraminifera of the Middle Eocene to Lower Oligocene shallow-marine units in the northern and eastern parts of the Thrace Basin, NW Turkey. Turkish Journal of Earth Sciences 20: 793-845.

Lüttig, G, Steffens P (1976). Paleogeographical Atlas and Explanatory Notes for Turkey from the Oligocene to the Pleistocene. Hannover, Germany: Bundesanstalt für Geowissenschaften und Rohstoffe.

Martini E (1971) Standard Tertiary and Quaternary calcareous nannoplankton zonation. In: Farinacci A (editor). Proceedings of the 2nd International Conference Planktonic Microfossils. Rome, Italy: Tecnosci, pp. 739-785.

McArthur JM, Howarth RJ, Shields GA (2012). Strontium isotope stratigraphy. In: Gradstein FM, Ogg JG, Schmitz M, Ogg G (editors). The Geologic Time Scale. Amsterdam, the Netherlands: Elsevier, pp. 127-144.

Nikishin AM, Okay AI, Tüysüz O, Demirer A, Amelin N et al. (2015). The Black Sea basins structure and history: new model based on new deep penetration regional seismic data. Part 1: Basins structure and fill. Marine and Petroleum Geology 59: 638-655.

Ogg JG, Ogg G, Gradstein FM (2008). The Concise Geological Time Scale. Cambridge, UK: Cambridge University Press.

Okay AI, Altıner D, Kylander-Clark ARC (2019a). Major Late Cretaceous mass flows in central Turkey recording the disruption of the Mesozoic continental margin. Tectonics 38: 960-989.

Okay AI, Özcan E, Cavazza W, Okay N, Less G (2010). Basement types, Lower Eocene series, Upper Eocene olistostromes and the initiation of the southern Thrace Basin, NW Turkey. Turkish Journal of Earth Sciences 19: 1-25.

Okay AI, Özcan E, Hakyemez A, Siyako M, Sunal G et al. (2019b). The Thrace Basin and the Black Sea: the Eocene-Oligocene connection. Geological Magazine 156: 39-61.

Okay AI, Satır M, Tüysüz O, Akyüz S, Chen F (2001). The tectonics of the Strandja Massif: Variscan and mid-Mesozoic deformation and metamorphism in the northern Aegean. International Journal of Earth Sciences 90: 217-233.

Özcan E, Less G, Baldi-Beke M, Kollanyi K, Acar F (2009). Oligo-Miocene foraminiferal record (Miogypsinidae, Lepidocyclinidae and Nummulitidae) from the western Taurides (SW Turkey): Biometry and Implications for the Regional Geology. Journal of Asian Earth Sciences 34: 740-760.

Özcan E, Less G, Okay AI, Báldi-Beke M, Kollányi K et al. (2010). Stratigraphy and larger foraminifera of the Eocene shallow-marine and olistostromal units of the southern part of the Thrace Basin, NW Turkey. Turkish Journal of Earth Sciences 19: 27-77.

Özcan E, Okay AI, Bürkan KA, Yücel AO, Özcan Z (2018). Middle-Late Eocene marine record of the Biga Peninsula, NW Anatolia, Turkey. Geologica Acta 16: 163-187.

Özcan E, Yücel AO, Less G, Kaygili S, Ali N et al. (2019). Reticulate *Nummulites* (*N. fabianii* lineage) and age of the *Pellatispira*-beds of the Drazinda Formation, Sulaiman Range, Pakistan. International Journal of Paleobiology and Paleontology 2 (1): 000105.

Popov S, Rogl F, Rozanov AY, Steininger FF, Shcherba IG et al. (2004). Lithological-paleogeographic maps of Paratethys 10 maps Late Eocene to Pliocene. Courier Forschungsinstitut Senckenberg 250: 1-46.

Racey A (1995). Lithostratigraphy and larger foraminiferal (nummulitid) biostratigraphy of the Tertiary of northern Oman. Micropaleontology 41 (Suppl.): 1-123.

Rögl F (1999) Mediterranean and Paratethys. Facts and hypotheses of an Oligocene to Miocene paleogeography. Geolica Carpathica 50: 339-349.

Şafak U (2016). Ostracod fauna and environmental features of Tertiary (Paleogene-Neogene) deposits in Yedikule-Istanbul region. Bulletin of the Mineral Research and Exploration of Turkey 152: 39-61.

Sahy D, Condon DJ, Hilgen FJ, Kuiper KF (2017). Reducing disparity in radio-isotopic and astrochronology based time scales of the late Eocene and Oligocene. Paleoceanography 32: 1018-1035.

Sakınç M (1994). Karaburun (B İstanbul) denizel Oligosen'inin stratigrafisi ve paleontolojisi. Maden Tetkik ve Arama Dergisi 116: 9-14 (in Turkish).

Simmons MD, Bidgood MD, Connell PG, Ćorić S, Okay AI et al. (2020). Biostratigraphy and palaeoenvironments of the Oligocene succession (İhsaniye Formation) at Karaburun (NW Turkey). Turkish Journal of Earth Sciences 29: 28-63.

Siyako M (2006). Tertiary rock units of the Thrace Basin. Litostratigrafi Birimleri Serisi 2: 43-83 (in Turkish).

Siyako M, Huvaz O (2007). Eocene stratigraphic evolution of the Thrace Basin, Turkey. Sedimentary Geology 198: 75-91.

Sunal G, Satır M, Natal'in B, Topuz G, von der Schmidt O (2011). Metamorphism and diachronous cooling in a contractional orogen: the Strandja Massif, NW Turkey. Geological Magazine 148: 580-596.

Tulan E, Sachsenhofer RF, Tari G, Flecker R, Fairbank V et al. (2020). Source rock potential and depositional environment of Lower Oligocene rocks in the Karaburun area, Turkey. Turkish Journal of Earth Sciences 29: 64-84.

Turgut S, Türkaslan M, Perinçek D (1991). Evolution of the Thrace sedimentary basin and its hydrocarbon prospectivity. In: Spencer AM (editor). Generation, Accumulation, and Production of Europe's Hydrocarbons. Amsterdam, the Netherlands: European Association of Petroleum Geoscientists, pp. 415-437.

Türkecan A, Yurtsever A (2002). Geological Map of Turkey, İstanbul Sheet, Scale 1:500 000. Ankara, Turkey: General Directorate of the Mineral Research and Exploration (MTA).

Varol B, Baykal M, Ayyıldız T (2009). Sedimentological-stratigraphical evaluation of Tertiary carbonates (Soğucak Formation) of Thrace Basin (Bozcaada - Kıyıköy). Mineral Research and Exploration Bulletin 139: 1-15.

Yücel AO, Özcan E, Erbil Ü (2020). Latest Priabonian larger benthic foraminiferal assemblages at the demise of the Soğucak Carbonate Platform (Thrace Basin and Black Sea shelf, NW Turkey): implications for the shallow marine stratigraphy. Turkish Journal of Earth Sciences 29: 85-114.